

# Viscum album shares hydraulic traits but causes a water uncoupling despite the adjustments of its host Pinus sylvestris.

Domingo Sancho-Knapik<sup>1</sup>, Juan Pedro Ferrio<sup>2</sup>, Eustaquio Gil-Pelegri<sup>2</sup>, Ana López-Ballesteros<sup>1</sup>, and José Javier Peguero-Pina<sup>1</sup>

<sup>1</sup>Centro de Investigacion y Tecnologia Agroalimentaria de Aragon

<sup>2</sup>Consejo Superior de Investigaciones Cientificas

April 07, 2025

## Abstract

Excessive mistletoe (*Viscum album*) proliferation is considered dangerous for the survival of Scots pine (*Pinus sylvestris*) stands, as mistletoe increases their sensitivity to drought stress. In order to better understand this sensitivity, the aim of this study was to explore in depth the hydraulic and gas exchange performance of *V. album* in relation to its host *P. sylvestris* during summer drought. We selected one of the Scots pine southernmost habitats that features oro-Mediterranean climatic conditions. Here we measured hydraulic traits, xylem embolism, water potential, gas exchange, plant conductance and branch transpiration in non-infected and infected pine branches and mistletoe. We concluded that 1) both species have similar xylem specific hydraulic conductivity, leaf specific conductivity, vulnerability to drought-induced cavitation and plant conductance, but the higher transpiration of *V. album* resulted in more negative shoot water potentials that entailed a higher risk of xylem cavitation; 2) infected pine branches adjusted stem conductivity to the supported leaf area, that could explain the lack of differences in leaf specific conductivity, gas exchange, water potential and branch conductance with non-infected pine branches; and 3) despite the pine hydraulic adjustment, *V. album* caused a water uncoupling, exacerbated with soil water deficit, in infected pine branches above an infection threshold.

## 1 Introduction

*Viscum album* subsp. *austriacum* (Wiesb.) Vollm., commonly named mistletoe, is a hemiparasitic plant that hosts tree species from genera *Pinus* and *Picea* mainly across Europe (Zuber 2004, Dobbertin and Rigling 2006, Kollas et al. 2017, Szmidla et al. 2019, Lech et al. 2020). Its presence is common and necessary in ecosystems, since its fruits and leaves serve as food for different species of birds and insects (Zuber 2004). However, over the last few decades, it has been observed an excessive mistletoe proliferation, both in number and extension, that may become even more severe due to climate change warming (Szmidla et al. 2019). This proliferation is considered dangerous for the survival of the stands, becoming the most frequent cause of biotic damage in stands of Scots pine (*Pinus sylvestris* L.) (Dobbertin and Rigling 2006, Michel et al. 2018, Szmidla et al. 2019). Excessive mistletoe infection causes Scots pine crown degradation and transparency (Dobbertin and Rigling 2006, Rigling et al. 2010), pine radial growth decline (Sangüesa-Barreda et al. 2012, Yan et al. 2016), and significant growth reductions at the forest stand scale (Kollas et al. 2017). Mistletoe also increases the sensitivity of Scots pines to drought stress (Zuber 2004, Sangüesa-Barreda et al. 2012) by exacerbating growth reduction caused by water scarcity (Sangüesa-Barreda et al. 2013) and increasing the risk of drought-induced mortality when growing in xeric environments (Salih et al. 2016, Rigling et al. 2010).

Scots pine is a well-known isohydric tree species that maintains a tight leaf stomatal control under a water-saving strategy (Irvine et al 1998, Poyatos et al. 2008, Martínez-Vilalta et al. 2009). That is, for a very small decrease in predawn water potential reaching a mild water deficit status, Scots pine shows a strong

decrease in stomatal conductance to avoid water losses (Sancho-Knapik et al. 2017). Scots pine also holds other features that characterize water saver species (Peguero-Pina et al. 2020) such as low values of maximum stomatal conductance (Martín-Gómez et al. 2023) or hydraulic conductivity (Cochard, 1992). It also presents a high vulnerability to air embolism when compared to other conifers (Cochard 1992) indicating a relative low resistance to drought (Martínez-Vilalta and Piñol 2002, Peguero-Pina et al. 2011).

By contrast, *V. album* displays high values of stomatal conductance, similar to other parasitic plants, which implies high transpiration rates and increased water consumption (Schulze et al. 1984, Ullmann et al. 1985). Additionally, unlike Scots pine, mistletoe shows limited capacity for stomata regulation under soil water deficit conditions (Zuber 2004, Zweifel et al. 2012), that would classify *V. album* into the water spender strategy (Peguero-Pina et al. 2020). This high transpiration rate should entail the need for a large supply of water for both, mistletoe and pine stems, that may lead to a higher conductivity. Despite these studies, not much else is known about the ecophysiology of *V. album* in comparison with its host *P. sylvestris*. Furthermore, to the extent of our knowledge, there is a lack of information concerning the hydraulics of *V. album*; there are no studies about its hydraulic conductivity or its vulnerability to cavitation. We also lack in-depth ecophysiology studies linking gas exchange and hydraulic parameters in infected Scots pine branches, necessary for a better understanding of the increased pine decline due to the combination of mistletoe infection and drought.

The aim of our study was to explore in depth the hydraulic and gas exchange functioning of *V. album* in relation to its host *P. sylvestris* under two contrasting scenarios, without and with high soil water deficit conditions, to identify the consequences of mistletoe infection for the water balance of the tree. For this, we have selected one of the Scots pine southernmost habitats, the mountain ranges of the Iberian Peninsula (Matías and Jump 2012). Here, some of the Scots pine stands appear to be already sensitive to aridity (Galiano et al. 2010; Peguero-Pina et al. 2011; Sanz et al. 2014) so it would be worthy to investigate whether mistletoe exacerbates the effects of water stress on pine. Our first hypothesis is that *V. album*, as a supposed water spender, should have a higher hydraulic conductivity than the water saver *P. sylvestris*. If this hypothesis is not fulfilled, we would expect *V. album* to have a higher resistance to drought-induced cavitation as its high transpiration rates would entail an elevated drop in leaf water potential. Our second hypothesis is that a pine branch, that has a relatively low hydraulic conductivity, can hydraulically hold a small mistletoe infection (i.e. a low percentage of mistletoe leaf area), but the higher the infection, the higher the decoupling with the xylem of the pine branch. We also hypothesized that this decoupling would be much higher under soil water deficit conditions.

## 2 Materials and Methods

### 2.1 Experimental site

We selected a monospecific forest of *Pinus sylvestris* L. moderately infected with *Viscum album* L. subsp. *austriacum* (Wiesb.) Vollm. located in Orihuela del Tremedal (40,54° N, 1.66° W, 1466 m a.s.l., Teruel, Spain) in the south-eastern “Sistema Ibérico” range. This site features oro-Mediterranean climatic conditions, being characterized by cold winters and arid summers (Peguero-Pina et al. 2011). The experimental plot (100 x 50 m) included both non-infected and infected pines with mistletoe. Trees were 30-50 years old, 7 to 10 m tall, with a diameter at chest height between 20 and 40 cm, and did not show massive visual symptoms of decline. Trees were sparsely distributed (ca. 600 trees ha<sup>-1</sup>), allowing the existence of functional branches in the lower parts of the trees available for sampling and physiological measurements. Mistletoe age in these branches mostly ranged from 5 to 10 years old.

### 2.2 Stem hydraulic conductivity

The hydraulic conductivity ( $K_h$ , kg m s<sup>-1</sup> MPa<sup>-1</sup>) of stem segments was determined for 14 non-infected pines, 14 infected pine branches with different mistletoe infestation levels (ranging from 20 to 100% of mistletoe leaf area), and the corresponding 14 mistletoe plants. Branches from different pines were collected in the early morning and immediately re-cut them under water obtaining branch samples ca. 70 cm in length. Then, non-infected and infected (including mistletoes) branches were preserved in black plastic bags with the cut

ends under water and were carried to the lab. Once there, two segments of each non-infected pine branch, two segments of each infected pine branch and two segments of mistletoe (being segments ca. 1–3 cm long and up to 0.9 cm in diameter) were prepared as described in Mayr et al. (2002). It should be noted that for infected pine branches, one measured pine segment was located before mistletoe insertion (pre-insertion) and the other after mistletoe insertion (post-insertion, Fig. S1). Segments were cut under water, placed in a tubing similar to that described by Cochard et al. (1996) and connected to a digital mass flowmeter Liqui-Flow (Bronkhorst High-Tech, Ruurlo, The Netherlands) to determine the flow rate. Segments were perfused with distilled, degassed and filtered (0.22  $\mu\text{m}$ ) water containing 0.005% (v/v) Micropur (Katadyn Products, Wallisellen, Switzerland) to prevent microbial growth (Mayr et al 2006). The measurement pressure was set to 8 kPa. After the hydraulic measurement, the length of segments was measured to obtain  $K_h$ . Then, segments were perfused with cyanosine 2% (w/v), washed with distilled water and drought in stove (60°C, 12h). Cross sections of each segment were obtained with a razor blade, photographed using a stereoscopic microscope, and analyzed with the IMAGEJ analysis software (<https://imagej.net/>) to obtain the conductive xylem area. It is worth mentioning that mistletoe segment sections had a radial staining pattern with ca. 30% of the cross section stained (Fig. S2). The specific hydraulic conductivity ( $K_s$ ,  $\text{kg m}^{-1} \text{s}^{-1} \text{MPa}^{-1}$ ) was then calculated by dividing  $K_h$  by the conductive xylem area. Finally, the leaf-specific conductivity (LSC,  $\text{kg m}^{-1} \text{s}^{-1} \text{MPa}^{-1}$ ) was calculated by dividing  $K_h$  by the projected leaf area supported by the measured segment (Peguero-Pina et al. 2011). For segments of infected pine branches located in the mistletoe pre-insertion, LSC was calculated considering i) only the area of pine needles and ii) the sum of the area of pine and mistletoe leaves. Leaf area was obtained by scanning the leaves and using the IMAGEJ analysis software. Additionally, as a estimation of the infection level, the percentage of pine leaf area with respect to total supported leaf area was calculated for each branch, obtaining a value of 100% in non-infected pine branches and values ranging from 80% to 0% in infected branches.

### 2.3 Xylem embolism

Vulnerability to embolism was measured in non-infected pine branches and mistletoe stems by constructing vulnerability curves using the dehydration method (Tyree and Sperry, 1989). First, we collected 10 non-infected (from 10 different non-infected trees) and 10 infected (from 10 different infected trees) large pine branches (>1 m long) following the procedure described above. Once in the lab, branches were left in the dark by placing them inside cardboard boxes for water potential stabilization, and were allowed to dehydrate. Periodically, during the dehydration process, the stem hydraulic conductivity ( $K_h$ ) of a particular pine branch or mistletoe plant was measured (following the procedure described above) in which water potential ( $\Psi$ , MPa) had previously been measured with a Scholander pressure chamber. Each  $K_h$  value was divided by the cross-sectional area of the measured segment.  $K_h$  values with similar  $\Psi$  were averaged ( $\pm$  s.e.) and then normalized. The conductivity (%) was plotted as a function of  $\Psi$  for non-infected pine branches and mistletoe stems, obtaining two vulnerability curves. Pairs of data were adjusted by using a sigmoidal function and the 50% loss of hydraulic conductivity ( $P_{50}$ ) was obtained for each curve (Peguero-Pina et al. 2014).

### 2.4 Water potential measurements

Plant water potential measurements were performed during the vegetative season of 2023, once on June 20 (after the spring rains; from now on called Spring) and once on August 31 (during summer drought; from now on called Summer). First, plant water potential was measured at predawn ( $\Psi_{pd}$ ) with a Scholander pressure chamber following the methodological procedure described by Turner (1988). Measurements at predawn were performed in pine shoots of 4 infected trees. Second, between 10:00 and 12:00 h solar time, water potential was conducted on the same 4 infected pines, selecting in each tree, one non-infected branch and one infected branch (with ca. 10 to 20 % of mistletoe leaf area). Branches were sun exposed with fully developed shoots, located in the southern exposure of the lower canopy (ca. 1.70 m above ground). For each branch, two measurements of water potential were obtained, one in the basal part of the branch ( $\Psi_1$ ) and the other on the apical shoot ( $\Psi_2$ , Fig. S1).  $\Psi_1$  was obtained by measuring a shoot previously enclosed in darkness with aluminum paper for 30 min to avoid irradiance. With this enclosing procedure shoots stop transpiring and shoot water potential becomes equal to the stem potential. Concerning infected branches,  $\Psi$

$\Psi_1$  was obtained from the closest pine shoot (ca. 10 cm) located in the mistletoe pre-insertion. The distance between  $\Psi_1$  and  $\Psi_2$  was ca. 40 cm. Additionally, mistletoe shoot water potential ( $\Psi_3$ , Fig. S1) was also obtained from the infected branches by measuring one of the mistletoe apical shoots. Simultaneously to these midday water potential measurements, gas exchange was also performed on the same branches as described in the next section.

### 2.5 Leaf gas exchange and chlorophyll fluorescence measurements

Gas-exchange and chlorophyll fluorescence measurements were performed twice during the vegetative period of 2023, once on June 20 (after the spring rains; from now on called Spring) and once on August 31 (during summer drought; from now on called Summer), with an open gas exchange system (CIRAS-3, PP-Systems, Amesbury, MA, USA) fitted with an automatic universal leaf cuvette (PLC6-U, PP-Systems, Amesbury, MA, USA). The controlled cuvette  $\text{CO}_2$  concentration was  $400 \mu\text{mol mol}^{-1}$  and the saturating photosynthetic photon flux density was  $1200 \mu\text{mol m}^{-2} \text{s}^{-1}$ . The VPD inside the leaf cuvette was set to coincide with the atmospheric value (ca. 1.25 kPa). Measurements were performed in the morning (between 10:00 and 12:00 h solar time) on sun exposed, fully developed leaves, located in the southern exposure of the lower canopy (ca. 1.30 m above ground). Due to plant phenology, leaves measured in spring were one-year-old while leaves measured in summer were current-year mature leaves of ca. 2 months old. During each day, gas exchange measurements were performed at the same branches that the ones used for midday water potential measurements (see section above), prior to the shoot removing. Gas exchange was also measured on other 4 infected pine branches (with ca. 10 to 20 % of mistletoe leaf area) with the corresponding 4 mistletoe plants and on 4 non-infected pines. For comparison, non-infected pine branches of infected pines and non-infected pines were grouped as the same plant type: “non-infected pine”.

After steady state gas-exchange rate was reached, the stomatal conductance ( $g_s$ ,  $\text{mmol H}_2\text{O m}^{-2} \text{s}^{-1}$ ), the net assimilation rate ( $A_N$ ,  $\mu\text{mol CO}_2\text{m}^{-2} \text{s}^{-1}$ ), and the effective quantum yield of PSII ( $\varphi_{\text{PSII}}$ ) were obtained and recalculated to actual leaf area (Alonso-Forn et al. 2022; Martín-Gómez et al. 2023). Water use efficiency (WUE,  $\mu\text{mol CO}_2\text{mmol}^{-1} \text{H}_2\text{O}$ ) was calculated as the ratio between  $A_N$  and  $g_s$ . Photosynthetic electron transport rate ( $J_{\text{flu}}$ ,  $\mu\text{mol m}^{-2} \text{s}^{-1}$ ) was also calculated according to Krall and Edwards (1992), following the methodology described in Peguero-Pina et al. (2016). Finally, mesophyll conductance ( $g_m$ ,  $\mu\text{mol CO}_2\text{m}^{-2} \text{s}^{-1}$ ) and maximum velocity of carboxylation ( $V_{\text{cmax}}$ ,  $\mu\text{mol CO}_2\text{m}^{-2} \text{s}^{-1}$ ) were estimated according to the variable  $J$  method of Harley et al. (1992) and the one-point method of De Kauwe et al. (2016), as described in Alonso-Forn et al. (2022).

During gas exchange measurements, air temperature and relative humidity were recorded using a Hobo Pro RH/Temp data logger (Onset Computer Bourne, MA, USA) located inside a solar shield 1.50 m above ground. The *in situ* leaf transpiration rate ( $E$ ,  $\text{mmol H}_2\text{O m}^{-2} \text{s}^{-1}$ ), i.e. the transpiration rates under outdoor conditions, was then recalculated as the product between measured  $g_s$  and the ambient  $[\text{?}]_w$ , being  $[\text{?}]_w$  the driving force for evaporation, i.e. the molar gradient in water vapor from the intercellular spaces in the leaf to the atmosphere (Percy et al. 1989).

### 2.6 Quantitative limitations analysis of $A_N$

The relative controls on  $A_N$  were separated into their functional components based on the quantitative limitation analysis by Grassi and Magnani (2005) as used in Tomás et al. (2013). This methodology facilitates the comparison of relative changes in restrictions to net  $\text{CO}_2$  assimilation into limitations due to leaf biochemistry (biochemical limitations,  $l_b$ ),  $g_m$  (mesophyll limitations,  $l_m$ ) and limited  $g_s$  to  $\text{CO}_2$  (stomatal limitations,  $l_s$ ). Each of the three components,  $l_b$ ,  $l_m$  and  $l_s$ , can range from zero to one, being the sum of the three equal to one ( $l_b + l_m + l_s = 1$ ). Equations for their calculation can be found in Alonso-Forn et al. (2022).

### 2.7 Pine branch and mistletoe conductance

Branch/plant conductance ( $k$ ,  $\text{mmol H}_2\text{O m}^{-2} \text{s}^{-1} \text{MPa}^{-1}$ ) was calculated for each experimental day for non-infected and infected pine branches, and for mistletoe plants as the ratio between  $E$  and  $[\text{?}]\Psi$  (Cochar

et al., 2000):

$$k = E / [?] \Psi$$

Where  $E$  is the *in situ* transpiration of the apical shoot and  $[?] \Psi$  is the water potential gradient. For pine branches,  $[?] \Psi$  was calculated as  $(\Psi_1 - \Psi_2)$ ; for mistletoe plants  $[?] \Psi$  was calculated as  $(\Psi_1 - \Psi_3)$ , where  $\Psi_1$  is the pine midday stem water potential, and  $\Psi_2$  and  $\Psi_3$  are the apical shoot midday water potential of pine and mistletoe, respectively (Fig. S1).

### 2.8 Branch transpiration rate

We calculated the branch transpiration rate ( $E_{\text{branch}}$ , mmol H<sub>2</sub>O s<sup>-1</sup>) by upscaling the mean values of recalculated in-situ transpiration ( $E$ ) to the branches used for determining the hydraulic conductivity ( $K_h$ ). For non-infected pines,  $E_{\text{branch}}$  was the product between  $E$  of non-infected pines and the pine leaf area (LA) supported by the branch ( $E_{\text{pine}} \times \text{LA}_{\text{pine}}$ ). For the measurements located before mistletoe insertion (pre-insertion) of infected branches,  $E_{\text{branch}}$  was the sum of i) the product between  $E$  of infected pines and the pine leaf area supported by the branch, and ii) the product between  $E$  of mistletoe and the mistletoe leaf area supported by the branch ( $E_{\text{pine}} \times \text{LA}_{\text{pine}} + E_{\text{mistletoe}} \times \text{LA}_{\text{mistletoe}}$ ). For mistletoe post-insertion measurements,  $E_{\text{branch}}$  was calculated as  $E_{\text{pine}} \times \text{LA}_{\text{pine}}$ . Afterwards,  $E_{\text{branch}}$  was plotted as a function of  $K_h$  for non-infected and infected pine branches using the  $E$  values obtained in spring and summer.

### 2.9 Statistical analysis

All statistical analyses were performed in *R v4.4.1* (R core team 2024). For stem diameter and leaf hydraulic variables, we tested significant differences between “Plant material” (non-infected pine, infected pine -pre-insertion-, infected pine -post-insertion- and mistletoe) using the built-in functions *lm* and *anova* from package *stats v.4.4.1* (R core team 2024). In the particular case of LSC, infected pine -pre insertion- was subdivided in two, one value calculated using only pine leaf area (p LA) and another using both pine and mistletoe leaf area (p+m LA). We also performed a paired *t*-test to test significant differences in these hydraulic variables between infected pine -pre-insertion- and infected pine -post-insertion-, reducing the variability.

For gas exchange variables and *in situ* plant conductance, we included “tree” as a random term in the models, using the *lmer* function from package *lme4 v. 1.1-35.5* (Bates et al. 2015). We first tested significant differences between “Season” (Spring, without water deficit; Summer, with water deficit), “Infection” (non-infected pine, infected pine) and their interaction (“Season × Infection”). Later on, we tested the effect of “Season”, “Species” (Pine; Mistletoe) and their interaction (“Season × Species”). Although neither “Infection” nor the “Season × Infection” terms were significant, for the comparison between species we used only the values for infected pines. By doing this, we selected the pine samples growing closest to mistletoe, and kept more homogenous group sizes for statistical analyses.

Over- and under-dispersion of model residuals was checked, including outlier tests, using the *simulateResiduals* function from package *DHARMA v.0.4.6* (Hartig 2022). Only minor issues were detected, which were solved with the log-transformation (for  $K_h$ ,  $LSC$ ,  $gs$ ,  $WUE$ ,  $gm$ ,  $E$  and  $[?] \Psi$ ). When required, multiple comparisons were assessed with the Tukey test ( $\alpha = 0.05$ ) using the function *emmeans* from package *emmeans v1.10.3* (Lenth 2022). Unless otherwise stated, means are shown together with their associated standard error of the mean.

## 3 Results

### 3.1 Hydraulic conductivity

Table 1 and Figure 1 show the values of stem diameter and hydraulic traits measured in non-infected pines, infected pine branches (pre- and post- insertion) and mistletoe. Stem diameter was statistically higher ( $P < 0.05$ ) for segments of infected pine branches measured in the mistletoe pre-insertion when compared with any other plant material considered, which did not show statistically significant differences among them at  $P < 0.05$  (Table 1, Fig. 1A). Hydraulic conductivity ( $K_h$ ) was statistically lower ( $P < 0.05$ ) for mistletoe

(Table 1, Fig 1B). The paired comparison between infected pine pre- and post- insertion revealed significant differences ( $P < 0.05$ ) in the stem diameter and  $K_h$  that were 1.6-fold and 3.3-fold higher, respectively, in infected pine pre-insertion. The difference in  $K_h$  between pre- and post- insertion resulted higher as mistletoe leaf area increased (Fig. 2A), indicating a hydraulic response in the pine to increases in mistletoe infection. There was not any statistical difference ( $P < 0.05$ ) in the values of specific hydraulic conductivity ( $K_s$ ) (Table 1, Fig. 1C). However, we found that  $K_s$  for segments of infected pine branches measured in the mistletoe post-insertion decreased statistically ( $P < 0.05$ ) with decreases in the percentage of pine leaf area of the branch (Fig. 2B). This relation was not significant for pine segments measured in the mistletoe pre-insertion (Fig. 2B). Regarding leaf specific conductivity (LSC), we found that LSC for segments of infected pine branches located in the mistletoe pre-insertion and calculated considering only the area of pine leaves (called “Infected<sub>pre</sub> (p LA)” in Fig. 1D), was statistically higher ( $P < 0.05$ ) than the other values (Table 1). These LSC values of “Infected<sub>pre</sub> (p LA)” were plotted as a function of the percentage of pine leaf area supported by the branch, showing an exponential increase in LSC as the percentage of pine leaf area decrease (Fig. 2C). By contrast, when LSC was calculated considering the sum of pine and mistletoe leaf areas (called “Infected<sub>pre</sub> (p+m LA)” in Fig. 1D), the mean value of LSC resulted not statistically different from the other pine materials (Table 1). Fig. 2C also shows higher values of LSC for pine segments located in the post-insertion of branches with percentage pine leaf area lower than 20%.

The curves of vulnerability to cavitation for non-infected pine and mistletoe stems are shown in Fig. 3. Both curves overlap for water potentials values between 0 and -1.5 MPa and from -3.5 to -4.5 MPa. For the rest of the values (between -1.5 and -3.5 MPa), the percentage of loss of conductivity for pine was slightly higher than for mistletoe. The sigmoidal adjustments showed that the water potentials at which the 50% loss of hydraulic conductivity occurs ( $P_{50}$ ) were  $-3.08 \pm 0.12$  MPa for pine and  $-2.45 \pm 0.16$  for mistletoe (Fig. 3). Although the estimated  $P_{50}$  was slightly lower for pine, the 95% confidence intervals of this parameter showed overlap between species (pine: [-3.36, -2.71]; mistletoe: [-2.74, -1.96]), indicating that the differences were not significant. Full model parameters are given in Supp. File 3 “Extended Statistics”.

### 3.2 *In situ gas exchange measurements*

Gas exchange parameters did not show significant differences between infected and non-infected pines, nor a significant season x infection interaction (Fig. 4, Table S1). Conversely, we found a strongly significant effect of season on stomatal conductance ( $g_s$ ) and water use efficiency (WUE) in pines (Fig. 4A,C). In spring, without soil water deficit,  $g_s$  for non-infected and infected pines were  $268 \pm 36$  and  $196 \pm 33$  mmol H<sub>2</sub>O m<sup>-2</sup>s<sup>-1</sup>, respectively; in summer, under soil water deficit, non-infected and infected pines showed lower  $g_s$  values:  $42 \pm 8$  and  $45 \pm 18$  mmol H<sub>2</sub>O m<sup>-2</sup> s<sup>-1</sup>, respectively. Comparing the two species (Table S2), mistletoe showed significantly higher  $g_s$  than pine across seasons, but a significant season x species interaction was found since the differences were much greater in summer. In contrast to the pine, mistletoe  $g_s$  did not show significant differences from spring to summer (Fig. 4A). The mistletoe did not show differences in net assimilation rate ( $A_N$ ), but showed a lower WUE than pine across seasons (Fig. 4B,C, Table S2). Similarly, we found significantly lower mesophyll conductance ( $g_m$ ), photosynthetic electron transport rate ( $J_{flu}$ ) and lower maximum velocity of carboxylation ( $V_{cmax}$ ) in mistletoe during spring, as compared to pine (Fig. 4D,E,F, Table S2). Surprisingly, mistletoe showed significantly higher values of  $g_m$  and  $J_{flu}$  in summer than in spring (Fig. 4D,E, Table S2). These unexpected results could be due to differences in the age of the measured leaves, rather than differences in water conditions: leaves measured in spring were ca. 12-months-old whereas leaves measured on summer (under soil water deficit) were ca. 2-months-old.

The quantitative limitations analyses of photosynthesis revealed that in spring, without water deficit,  $A_N$  was mainly limited by  $g_m$  in the three plant-material types considered (non-infected pine, infected pine and mistletoe, Fig. 5A). By contrast, in summer, under water deficit,  $A_N$  in non-infected and infected pines was limited mainly by  $g_s$ , whereas  $g_m$  remained the major limitation in mistletoe (Fig. 5B).

### 3.3 *Water potential, in-situ leaf transpiration rate and whole-branch conductance*

As expected, predawn water potential ( $\Psi_{pd}$ ) in spring was  $0.0 \pm 0.0$  MPa, confirming that plant measure-

ments were carried out without soil water deficit, whereas in summer the  $\Psi_{pd}$  dropped to  $-1.40 \pm 0.02$  MPa, indicating moderate soil water deficit conditions. Neither basal ( $\Psi_1$ ) nor apical ( $\Psi_2$ ) midday water potential in pines showed significant differences between infected and non-infected branches (Fig. 6A,B, Table S3). Similarly, the water potential gradient along the branch ( $[\Psi]$ ), recalculated *in-situ* leaf transpiration rate ( $E$ ) and whole-branch conductance ( $k$ ) were not significantly affected by mistletoe infection (Fig. 6C,D,E, Table S3). Conversely, we found strong seasonal differences in water potential and transpiration (Table S3). Both  $\Psi_1$  and  $\Psi_2$  were significantly lower (i.e. more negative) during summer, in agreement with the lower soil water availability. Similarly, the gradient  $[\Psi]$  and  $E$  of pines were significantly higher in spring than in summer (Fig. 6C,D). Consequently, the  $k$  of pines, as the quotient of  $E$  and  $[\Psi]$ , did not varied significantly from spring to summer (Fig. 6E, Table S3).

When comparing the two species, we found significant differences in the apical midday water potential for pine ( $\Psi_2$ ) and mistletoe ( $\Psi_3$ ), the latter being more negative across seasons (Fig. 6AB, Table S4). Unlike in pines, differences between spring and summer  $\Psi_3$  were not significant in mistletoe (Fig. 6A,B). As a result, the gradient  $[\Psi]$  was significantly higher in mistletoe compared to pines for both seasons and did not vary significantly from spring to summer (Fig. 6C, Table S4). With regard to  $E$ , the mistletoe kept high values across the two seasons (no significant differences), being significantly higher than pine (Fig. 6D, Table S4). Notably, despite the higher  $E$ , the  $k$  of mistletoe was not significantly different from the  $k$  of pine (Fig. 6E, Table S4). Finally, the overall seasonal trend for  $k$  also did not show significant differences between spring and summer within each species (Fig. 6E, Table S4).

### 3.4 Association between branch transpiration rate and hydraulic conductivity

Individual branch transpiration ( $E_{branch}$ ) plotted as a function of hydraulic conductivity ( $K_h$ ) for pine branches obtained in spring and summer (without and under water deficit, respectively), is shown in figures 7A and 7C. These relationships for non-infected pines were adjusted to a linear model ( $R = 0.97$ ,  $P < 0.0001$ ), where increases in  $K_h$  are matched by increases in  $E_{branch}$  (Figs. 7A,C). Plotted values for infected pine branches obtained from mistletoe post-insertion overlap this linear model, while those obtained from mistletoe pre-insertion are mostly segregated from the linear model, specially noticed under water deficit conditions (Fig. 7C). A value of segregation from the linear model for each infected plotted point was calculated as the difference between measured  $E_{branch}$  and predicted  $E_{branch}$ , and then plotted as a function of the percentage of mistletoe leaf area of the branch (Figs. 7B,D). We found that the higher the percentage of mistletoe leaf area in the branch, the higher the segregation from the non-infected linear model (i.e. the higher the difference between measured  $E_{branch}$  and predicted  $E_{branch}$ ; Fig 7). For instance, if we consider an infected branch with a stem  $K_h$  value of  $1 \times 10^{-5} \text{ kg m s}^{-1} \text{ MPa}^{-1}$  that has a 50% of mistletoe leaf area, we should expect a branch transpiration 4-fold higher than in a non-infected branch with the same value of  $K_h$ . In addition, the 95% prediction intervals (Figs. 7A,C) give us an upper limit that can be associated to the maximum percentage of mistletoe leaf area a pine branch can hold without surpassing this upper limit in terms of branch transpiration. This threshold allows us to identify when the coupling between  $K_h$  and transpiration observed for non-infected branches is no longer maintained. Thus, for spring (without water deficit), the maximum percentage of mistletoe leaf area for not surpassing the 95% upper prediction interval would be 46%, while for summer (under water deficit) it would be only 11%.

## 4 Discussion

### 4.1 Hydraulic and gas exchange properties of Scots pine and *Viscum album*: similarities and differences

The water saver Scots pine showed in this study values of specific hydraulic conductivity ( $K_s$ ), leaf specific conductivity (LSC), and water potential inducing 50% loss of hydraulic conductivity ( $P_{50}$ ) within the range of the species (Cochard et al. 1992, Martínez-Vilalta et al. 2008). Surprisingly, *Viscum album* did not differ significantly from Scots pine in either these variables or plant conductance ( $k$ ), indicating similar xylem specific hydraulic properties and vulnerability to cavitation, as compared to its host. According to Zhang et al. (2024), mistletoes and their respective host species have similar values of hydraulic-related variables in wet habitats, and the values become different when habitats become drier, which would indicate that our

data confirm that Scots pine is more associated with humid rather than arid environments. In any case, we must reject our first hypothesis where we had considered *Viscum album* as a species with a higher hydraulic conductivity and a higher resistance to drought-induced cavitation than Scots pine. Having a similar  $K_s$ , LSC and  $k$  as Scots pine but with a higher transpiration rate, caused in mistletoe a larger drop in midday water potential as compared to the pine (Fig. 6), similarly to the results of Zweifel et al. (2012). Moreover, this water potential drop reached values around the  $P_{50}$  for mistletoe, resulting in a very narrow safety margin. Conversely, Scots pine achieved a greater safety margin, typical of isohydric species (Martín-Gómez et al. 2017).

The higher transpiration rate found in *V. album*, which is common in mistletoe species (Schulze et al. 1984, Ullmann et al. 1985), was first suggested to be necessary for mistletoe to collect sufficient nitrogen from the xylem of the host (Schulze et al. 1984). Subsequently, Zuber (2004) suggested that a higher transpiration entailed a higher internal  $\text{CO}_2$  concentration in the leaf mesophyll, which agrees our results. The higher transpiration found in our study for mistletoe resulted from a higher stomatal conductance ( $g_s$ , Fig. 4), that entails a better capacity to increase substomatal  $\text{CO}_2$  concentration. In this way, *V. album* compensated for its lower mesophyll conductance ( $g_m$ ), lower photosynthetic electron transport rate ( $J_{\text{flu}}$ ) and lower maximum velocity of carboxylation ( $V_{\text{cmax}}$ ) (Fig. 4) by increasing carbon availability in the mesophyll. As a result, *V. album* reached similar net assimilation rates than Scots pine but at the expense of a higher water consumption, which implied a lower water use efficiency (WUE) that indicates a more aggressive water use (Zhang et al. 2012).

#### 4.2 Adjustments in Scots pine branches induced by *Viscum album*

We found significantly larger stem diameters in infected pine segments measured at the pre-insertion of mistletoe infection when compared to segments measured at the post-insertion (Table 1, Fig S1). This host branch hypertrophy was already reported in one of the first mistletoe anatomy studies (Smith and Gledhill, 1983) and recently confirmed by Mylo et al. (2021), who also showed a positive linear correlation with mistletoe age. Our study also demonstrated that the larger diameter measured at the pre-insertion entailed a higher hydraulic conductivity ( $K_h$ ). Moreover, the difference in  $K_h$  between pre- and post- insertion was positively correlated with mistletoe leaf area (Fig. 2A), indicating that Scots pine may increase  $K_h$  as a response of mistletoe growth and development. Besides, when only considering the pine leaf area to calculate the pine leaf specific conductivity (LSC) in the pre-insertion, we obtained aberrantly high values (Fig. 1D) that increased with increases in mistletoe leaf area (Fig. 2C). This indicated an excessive disproportion of pine  $K_h$  for the given pine leaf area, not fulfilling the so-called “pipe model theory” (Shinozaki et al. 1964) that considers the conductive portion of a stem to be proportional to the supported foliage (Lehnebach et al. 2018). However, when including the mistletoe leaf area in the pine pre-insertion LSC calculation, the resulting values were consistent with those of a non-infected pine (Table 1, Fig. 1), adjusting to the pipe model theory. That is, Scots pine adapts stem conductivity to supported leaf area and for this reason we found no differences in LSC between non-infected and infected pine branches. Regarding to this, Meinzer et al. (2004) also found no differences in LSC between non-infected and infected branches in western hemlock (*Tsuga heterophylla*) infected with hemlock dwarf mistletoe (*Arceuthobium tsugense*), which was explained with reductions in the hemlock leaf area of infected branches. We also observe this phenomenon in the post-infection measurements of the most infected pine branches (< 20% of pine leaf area, Fig. 2C) as we noticed unusually high values of LSC for similar stem diameters, indicating the reduction in leaf area. Meinzer et al. (2004) also stated that LSC was not different between non-infected and infected branches because the leaf area to sapwood area ratio of infected branches was lower, which is consistent with our results (data not shown). By contrast, unlike Meinzer et al. (2004), we did not find statistical differences in specific hydraulic conductivity ( $K_s$ ) between non-infected and infected branch xylems. However, we found a gradual reduction in  $K_s$  in the post-infection pine segments (Fig. 2B), indicating a progressive reduction in water transport efficiency only in the pine xylem located in the mistletoe post-insertion.

Concerning gas exchange, we did not find evidences of a potential impact of mistletoe on photosynthetic parameters of Scots pine. Overall, although lower values were generally obtained in infected pine branches,

neither  $g_s$ ,  $g_m$ ,  $A_N$  nor WUE were significantly different between non-infected and infected pine branches (Fig. 4). We also did not find significant differences in the basal and apical midday water potentials, nor in the transpiration rate or in the branch conductance (Fig. 6). Therefore, the ability for CO<sub>2</sub> assimilation of Scots pine is not necessarily diminished by the existence of mistletoe. Scalon et al. (2021) also found no significant differences in gas exchange and midday leaf water potential values when studying the mistletoe *Passovia ovata* on the evergreen host *Miconia albicans* during the dry season. However, differences in these variables in the wet season were statistically significant in Scalon et al. (2021), unlike our results. A reason for the absence of differences between non-infected and infected branches in our study could be the existence of adjustments in hydraulic architecture of infected pines that maintained LSC (discussed above), which contribute to sustaining  $g_s$ , leaf transpiration and shoot water potential (Meinzer et al. 2004). These results should be carefully interpreted, as gas exchange measurements were carried out in infected branches with little mistletoe infection (between 10 to 20% of mistletoe leaf area). Further measurements should be performed in branches with a higher degree of mistletoe infection to accurately elucidate the potential negative effect of mistletoe over the photosynthetic activity of host plant.

#### 4.3 Response to summer drought

The main effect of soil water scarcity during summer observed in Scots pine was the reduction in  $g_s$ , that reduced branch transpiration and the value of the water potential gradient between the base and the apex of the branch (Figs. 4, 6). The limited impact of drought over other photosynthetic traits such as  $g_m$  and  $V_{cmax}$  implied that the main relative limitations to photosynthesis changed from mesophyll limitations ( $l_m$ ) during spring (without drought) to stomatal limitations ( $l_s$ ) during summer drought (Fig. 5). By contrast, mistletoe did not experience changes in  $g_s$  with soil water deficit, and thus, we found no significant changes in transpiration, in the apical shoot midday water potential, in the water potential gradient, nor in the relative limitations to photosynthesis between spring and summer (Figs. 4, 5, 6). Unlike Scots pine, which is well known to reduce  $g_s$  with increasing soil water deficit (e.g. Sancho-Knapik et al. 2017), *V. album* barely regulates its stomata (Zweifel et al. 2012), even when experiencing water potential values (Fig. 6) close to its  $P_{50}$  (Fig. 3). However, stomatal responses of *V. album* to environmental changes do exist (Zuber 2004). Previous studies reported that  $g_s$  in *V. album* showed large and consistent changes associated with variations in vapor pressure deficit and temperature (Ullmann et al. 1985, Zweifel et al. 2012), although these changes were negligible in our study.

Concerning the association between branch transpiration rate ( $E_{branch}$ ) and hydraulic conductivity ( $K_h$ ), non-infected pine branches showed a hydraulic balance between the water input through the xylem and the water output via transpiration, resulting in a strong linear correlation between  $K_h$  and  $E_{branch}$  (Fig 7). Infected pine branches measured at the post-insertion of the mistletoe maintained this hydraulic balance as their values overlap the non-infected ones. However, we found a hydraulic uncoupling, specially noticed during summer drought, in the mistletoe pre-insertion of infected pine branches as, for a given  $K_h$ ,  $E_{branch}$  was much higher than for non-infected pines. That is, the existence of mistletoe causes the whole infected branch to transpire above its supplying possibilities, causing a hydraulic uncoupling. It must be highlighted that this phenomenon is exacerbated with the increase of mistletoe infection and soil water deficit. This hydraulic uncoupling could be buffered by increasing pine stem diameter, adapting conductivity to leaf area demand (see above for discussion). However, the hydraulic uncoupling is not completely avoided. According to the interpretation of our results, during spring (without water deficit) the maximum percentage of mistletoe leaf area that can be supported by a pine branch without having a hydraulic uncoupling is 46%, while for summer (under moderate water deficit) is only 11%. Therefore, a pine branch can support a mistletoe plant without further hydraulic consequences when the mistletoe leaf area is under these percentages, confirming our second hypothesis.

## 5 Conclusion

The comparison between Scots pine and *Viscum album* reveals that both species have the same xylem specific hydraulic properties and similar vulnerability to cavitation. However, the higher transpiration of *V. album* resulted in a higher drop in shoot water potential that entailed a very narrow safety margin to avoid xylem

cavitation, unlike the wider safety margin of Scots pine.

The infection of *V. album* induces hydraulic adjustments in pine branches to cope with the higher water demand. In particular, we found larger stem diameters and a higher hydraulic conductivity in the pre-insertion of infected pine branches, and a reduction in the leaf area of pine branches. By adjusting stem conductivity to the supported leaf area, infected pine branches showed the same leaf specific conductivity as non-infected branches. This adjustment could also have explained the lack of differences in other measured variables such as stomatal conductance, net assimilation rate, midday water potential or branch conductance.

The higher stomatal conductance of *V. album* may increase its ability for CO<sub>2</sub> assimilation, partially compensating for its lower mesophyll conductance and biochemical rates. The high transpiration of *V. album* causes a water uncoupling in infected pine branches above a certain infection level, despite the hydraulic adjustments of Scots pine branches. Soil water deficit reduces stomatal conductance and branch transpiration in Scots pine, but not in *V. album*, exacerbating the water uncoupling in infected branches.

## 6 Acknowledgements

This research was funded by Gobierno de Aragón-Fondo de Inversiones de Teruel (FITE) and Gobierno de España, grant project FITE-2021-DRUIDA and by Gobierno de Aragón research group S74.23R. Work of ALB was supported by a Juan de la Cierva-Incorporación postdoctoral contract IJC2020-045630-I funded by MCIN/AEI /10.13039/501100011033 and by European Union NextGenerationEU/PRTR.

## 7 References

- Alonso-Forn D, Peguero-Pina JJ, Ferrio JP, Garcia-Plazaola JI, Martin-Sanchez R, Niinemets U, Sancho-Knapik D, Gil-Pelegrin E (2022) Cell-level anatomy explains leaf age-dependent declines in mesophyll conductance and photosynthetic capacity in the evergreen Mediterranean oak *Quercus ilex* subsp. *rotundifolia*. *Tree Physiol.* 42:1988–2002
- Bates D, Maechler M, Bolker B, Walker S (2015). Fitting Linear Mixed-Effects Models Using lme4. *J. Stat. Softw.* 67:1-48.
- Cochard H (1992) Vulnerability of several conifers to air embolism. *Tree Physiol.* 11:73-83.
- Cochard H, Breda N, Granier A (1996) Whole tree hydraulic conductance and water loss regulation in *Quercus* during drought: Evidence for stomatal control of embolism? *Ann. For. Sci.* 53:197–206.
- Cochard H, Martin R, Gross P, Bogeat-Triboulot M. 2000. Temperature effects on hydraulic conductance and water relations of *Quercus robur* L. *J. Exp. Bot.* 51:1255–1259.
- Dobbertin M, Rigling A (2006) Pine mistletoe (*Viscum album* ssp. *austriacum*) contributes to Scots pine (*Pinus sylvestris*) mortality in the Rhone valley of Switzerland. *For. Path.* 36:309–322.
- Galiano L, Martinez-Vilalta J, Lloret F (2010) Drought-induced multifactor decline of Scots pine in the Pyrenees and potential vegetation change by the expansion of co-occurring oak species. *Ecosystems* 13:978–991.
- Irvine J, Perks MP, Magnani F, Grace J (1998) The response of *Pinus sylvestris* to drought: stomatal control of transpiration and hydraulic conductance. *Tree Physiol.* 18:393-402.
- Kollas C, Gutsch M, Hommel R, Lasch-Born P, Suckow F (2017) Mistletoe-induced growth reductions at the forest stand scale. *Tree Physiol.* 38:735-744.
- Lech P, Zolciak A, Hildebrand R (2020) Occurrence of European mistletoe (*Viscum album* L.) on forest trees in Poland and its dynamics of spread in the period 2008–2018. *Forests* 11:83.
- Lehnebach R, Beyer R, Letort V, Heuret P (2018) The pipe model theory half a century on: a review. *Ann. Bot.* 121:773–795.

- Matías L, Jump AS (2012) Interactions between growth, demography and biotic interactions in determining species range limits in a warming world: The case of *Pinus sylvestris*. *For. Eco. Manag.* 282:10-22.
- Martín-Gómez P, Aguilera M, Pemán J, Gil-Peigrín E, Ferrio JP (2017) Contrasting ecophysiological strategies related to drought: the case of a mixed stand of Scots pine (*Pinus sylvestris*) and a submediterranean oak (*Quercus subpyrenaica*). *Tree Physiol.* 37:1478–1492.
- Martín-Gómez P, Rodríguez-Robles U, Ogée J, Wingate L, Sancho-Knapik D, Peguero-Pina JJ, dos Santos Silva JV, Gil-Peigrín E, Pemán J, Ferrio JP (2023) Contrasting stem water uptake and storage dynamics of water-saver and water-spender species during drought and recovery. *Tree Physiol.* 43:1290–1306.
- Martínez-Vilalta J, Piñol J (2002) Drought-induced mortality and hydraulic architecture in pine populations of the NE Iberian Peninsula. *For. Ecol. Manag.* 161:247–256
- Martínez-Vilalta J, Cochard H, Mencuccini M, Sterck F, Herrero A, Korhonen JFJ, Llorens P, Nikinmaa E, Nolè A, Poyatos R, Ripullone F, Sass-Klaassen U, Zweifel R (2009) Hydraulic adjustment of Scots pine across Europe. *New Phytol.* 184:353-364.
- Mayr, S., M. Wolfschwenger and H. Bauer. 2002. Winter-drought induced embolism in Norway spruce (*Picea abies*) at the Alpine timberline. *Physiol. Plant.* 115:74–80.
- Mayr, S.; Wieser, G.; Bauer, H. Xylem temperatures during winter in conifers at the alpine timberline. *Agric. For. Meteorol.* 2006, 137, 81–88.
- Michel A, Seidling W, Prescher AK (2018) Forest Condition in Europe: 2018. Technical Report of ICP Forests. Report under the UNECE Convention on long-range transboundary air pollution (Air Convention); BFW-Dokume: Vienna, Austria.
- Mylo MD, Hofmann M, Delp A, Scholz R, Walther F, Speck T, Speck O (2021) Advances on the visualization of the internal structures of the European mistletoe: 3D reconstruction using microtomography. *Front. Plant Sci.* 12:715711.
- Pearcy RW, Schulze ED, Zimmermann R (1989) Measurement of transpiration and leaf conductance in plant physiological ecology, eds Pearcy RW, Ehleringer J, Mooney HA, Rundel PW (London: Chapman and Hall), 137–160.
- Peguero-Pina JJ, Alquézar-Alquézar JM, Mayr S, Cochard H, Gil-Peigrín E (2011) Embolism induced by winter drought may be critical for the survival of *Pinus sylvestris* L. near its southern distribution limit. *Ann. For. Sci.* 68:565–574.
- Peguero-Pina JJ, Sisó S, Fernández-Marín B, Flexas J, Galmés J, García-Plazaola J I, Niinemets Ü, Sancho-Knapik D, Gil-Peigrín E (2016) Leaf functional plasticity decreases the water consumption without further consequences for carbon uptake in *Quercus coccifera* L. under Mediterranean conditions. *Tree Physiol.* 36:356–367.
- Peguero-Pina JJ, Vilagrosa A, Alonso-Forn D, Ferrio JP, Sancho-Knapik D, Gil-Peigrín E (2020). Living in drylands: functional adaptations of trees and shrubs to cope with high temperatures and water scarcity. *Forests* 11:1028.
- Poyatos R, Llorens P, Piñol J, Rubio C (2008) Response of Scots pine (*Pinus sylvestris* L.) and pubescent oak (*Quercus pubescens* Willd.) to soil and atmospheric water deficits under Mediterranean mountain climate. *Ann. For. Sci.* 65:306.
- R Core Team (2024). R: A Language and Environment for Statistical Computing. R Foundation for Statistical Computing, Vienna, Austria.
- Rigling A, Eilmann B, Koechli R, Dobbertin M (2010) Mistletoe-induced crown degradation in Scots pine in a xeric environment. *Tree Physiol.* 30:845-852.

Salih Mutlu S, Osma E, Ilhan V, Turkoglu HI, Atici O (2016) Mistletoe (*Viscum album*) reduces the growth of the Scots pine by accumulating essential nutrient elements in its structure as a trap. *Trees* 30:815–824.

Sancho-Knapik D, Sanz MA, Peguero-Pina JJ, Niinemets Ü, Gil-Peigrín E (2017) Changes of secondary metabolites in *Pinus sylvestris* L. needles under increasing soil water deficit. *Ann. For. Sci.* 74:24.

Sangüesa-Barreda G, Linares JC, Camarero JJ (2012) Mistletoe effects on Scots pine decline following drought events: insights from within-tree spatial patterns, growth and carbohydrates. *Tree Physiol.* 32:585–598.

Sangüesa-Barreda G, Linares JC, Camarero JJ (2013) Drought and mistletoe reduce growth and water-use efficiency of Scots pine. *For. Eco. Manag.* 296:64–73.

Sanz MA, Sánchez J, Camarero JJ, Peguero-Pina JJ, Sancho-Knapik D, Gil-Peigrín E (2014) Change in the terpenoid profile and secondary growth in declining stands of *Pinus sylvestris* L. under Mediterranean influence as a response to local factors. *Pirineos* 169:e003.

Scalon MC, Rossatto DR, Franco AC (2021) How does mistletoe infection affect seasonal physiological responses of hosts with different leaf phenology? *Flora* 281:151871.

Schulze E, Turner D, Glatzel G (1984) Carbon, water and nutrient relations of two mistletoes and their hosts: A hypothesis. *Plant Cell Environ.* 7:293–299.

Shinozaki K, Yoda K, Hozumi K, Kira T (1964) A quantitative analysis of plant form – the pipe model theory. II. Further evidence of the theory and its application in forest ecology. *Jpn. J. Ecol.* 14: 133–139.

Smith PL, Gledhill D (1983). Anatomy of the endophyte of *Viscum album* L. (Loranthaceae). *Bot. J. Linn. Soc.* 87, 29–53.

Szmidla H, Tkaczyk M, Radosław Plewa R, Tarwacki G, Sierota Z (2019) Impact of common mistletoe (*Viscum album* L.) on Scots pine forests—A call for action. *Forests* 10:847.

Tyree MT, Sperry JS. 1989. Vulnerability of xylem to cavitation and embolism. *Annu. Rev. Plant Physiol. Plant Mol. Biol.* 40:19–38.

Ullmann I, Lange OL, Ziegler H, Ehleringer J, Schulze E, Cowan IR (1985) Diurnal courses of leaf conductance and transpiration of mistletoes and their hosts in Central Australia. *Oecol.* 67:577–587.

Yan CF, Gessler A, Rigling A, Dobbertin M, Han XG, Li MH (2016) Effects of mistletoe removal on growth, N and C reserves, and carbon and oxygen isotope composition in Scots pine hosts. *Tree Physiol.* 36:562–575.

Zhang YB, Huang XY, Corrêa Scalon M, Ke Y, Liu JX, Wang Q, Li WH, Yang D, Ellsworth DS, Zhang YJ, Zhang JL (2025) Mistletoes have higher hydraulic safety but lower efficiency in xylem traits than their hosts. *New Phytol.* 245: 607–624.

Zweifel R, Bangerter S, Rigling A, Sterck FJ (2012) Pine and mistletoes: how to live with a leak in the water flow and storage system? *J. Exp.Bot.* 63:2565–2578.

Zuber D (2004) Biological flora of Central Europe: *Viscum album* L. *Flora* 199:181–203.

## Tables

**Table 1** Stem diameter (mm) and hydraulic variables measured in non-infected pines (n=28), infected pines (pre- and post- mistletoe insertion, n=14) and mistletoe (n=28).

	Non-infected pine	Infected pine (pre-insertion)	Infected pine (post-insertion)	Mistletoe
Stem diameter	4.3 ±0.4 b	6.0 ±0.5 a	3.8 ±0.4 b*	3.2 ±0.2 b
$K_h \times 10^{-6}$	4.4 ±0.7 a	7.6 ±1.5 a	2.3 ±0.4 a*	0.75 ±0.13 b
$K_s$	0.29 ±0.02 a	0.25 ±0.02 a	0.21 ±0.02 a	0.22 ±0.02 a

	Non-infected pine	Infected pine (pre-insertion)	Infected pine (post-insertion)	Mistletoe	
LSC x 10 <sup>-5</sup>	7.6 ±0.4 bc	(p LA) 58 ±24 a	(p+m LA) 11.1 ±1.4 b	16.5 ±5.8 b	6.7 ±0.7

$K_h$ , hydraulic conductivity ( $\text{kg m s}^{-1} \text{MPa}^{-1}$ );  $K_s$ , specific hydraulic conductivity ( $\text{kg m}^{-1} \text{s}^{-1} \text{MPa}^{-1}$ ); LSC, leaf specific conductivity ( $\text{kg m}^{-1} \text{s}^{-1} \text{MPa}^{-1}$ ). LSC for infected pines (pre-insertion) has been calculated using only the pine leaf area (p LA) and considering the sum of both pine and mistletoe leaf areas (p+m LA). Values are means  $\pm$  s.e. Letters indicate statistically significant differences across plant-material types (Tukey test,  $P < 0.05$ ). Asterisks indicate significant differences between infected pine pre- and post- mistletoe insertion (paired  $t$ -test,  $P < 0.05$ ). Expanded statistics are given in Supp. File 3.

## Figures

**Fig. 1** Box-plot representation of the stem diameter (A), hydraulic conductivity ( $K_h$ , B), specific hydraulic conductivity ( $K_s$ , C) and leaf specific conductivity (LSC, D) measured in non-infected pines (orange, n=28), infected pines branches: mistletoe pre-insertion (infected<sub>pre</sub>, light grey, n=14) and post-insertion (infected<sub>post</sub>, dark grey, n=14), and mistletoe (blue, n=28). LSC for infected pines pre-insertion has been calculated using only pine leaf area (p LA) and the sum of pine and mistletoe leaf areas (p+m LA).

### Hosted file

image1.emf available at <https://authorea.com/users/817787/articles/1284115-viscum-album-shares-hydraulic-traits-but-causes-a-water-uncoupling-despite-the-adjustments-of-its-host-pinus-sylvestris>

**Fig. 2** Relationships between infection level and hydraulic traits. A: The difference between  $K_h$  measured pre- and post-insertion is plotted as a linear function of mistletoe leaf area. B and C: Relationships between the percentage of pine leaf area of the branch and specific hydraulic conductivity ( $K_s$ , B) and leaf specific conductivity (LSC, C) for infected pines branches: mistletoe pre-insertion (infected<sub>pre</sub>, light grey, dashed line) and post-insertion (infected<sub>post</sub>, dark grey, solid line). LSC for infected pines pre-insertion is calculated using only pine leaf area (p LA). The mean values of  $K_s$  and LSC for non-infected branches are also included in B and C, respectively.

### Hosted file

image2.emf available at <https://authorea.com/users/817787/articles/1284115-viscum-album-shares-hydraulic-traits-but-causes-a-water-uncoupling-despite-the-adjustments-of-its-host-pinus-sylvestris>

**Fig. 3** Curves of vulnerability to cavitation for non-infected *Pinus sylvestris* and *Viscum album* stems. Each point is the average ( $\pm$  s.e.) of 5-9 single measurements. Pairs of points were adjusted by using a sigmoidal function to estimate the potential at which the 50% loss of hydraulic conductivity occurs ( $P_{50}$ ; value  $\pm$  s.d. in -MPa for each species is shown in the graph).

### Hosted file

image3.emf available at <https://authorea.com/users/817787/articles/1284115-viscum-album-shares-hydraulic-traits-but-causes-a-water-uncoupling-despite-the-adjustments-of-its-host-pinus-sylvestris>

**Fig. 4** Gas exchange parameters for non-infected pine branches (orange), infected pine branches (grey) and mistletoe (blue), measured in spring and summer.  $g_s$ , stomatal conductance;  $A_N$ , net assimilation rate; WUE, water use efficiency;  $g_m$ , mesophyll conductance;  $J_{flu}$ , photosynthetic electron transport rate;  $V_{cmax}$ , maximum velocity of carboxylation. Data are means  $\pm$  s.e. (n=8). Asterisks indicate statistically significant differences across plant material types. ns, not significant. Letters indicate statistically significant differences across seasons (Tukey test,  $P < 0.05$ ).

### Hosted file

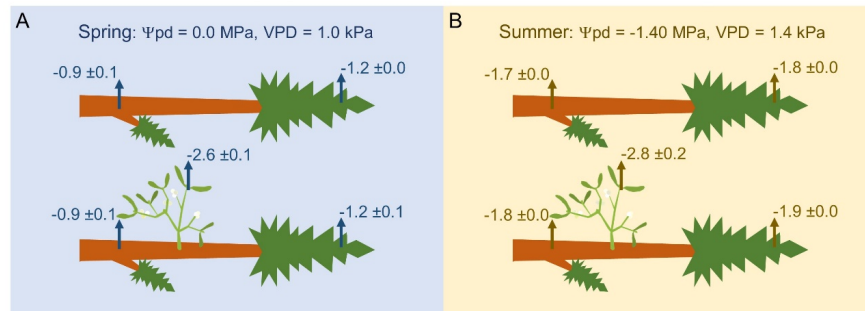
image4.emf available at <https://authorea.com/users/817787/articles/1284115-viscum-album-shares-hydraulic-traits-but-causes-a-water-uncoupling-despite-the-adjustments-of-its-host-pinus-sylvestris>

**Fig. 5** Relative limitations to photosynthesis ( $A_N$ ) in spring and summer calculated for non-infected pine branches, infected pine branches and mistletoe.  $l_b$ , biochemical limitations;  $l_m$ , mesophyll limitations;  $l_s$ , stomatal limitations. Asterisks indicate statistically significant differences across plant-material types (Tukey test,  $P < 0.05$ ).

### Hosted file

image5.emf available at <https://authorea.com/users/817787/articles/1284115-viscum-album-shares-hydraulic-traits-but-causes-a-water-uncoupling-despite-the-adjustments-of-its-host-pinus-sylvestris>

**Fig. 6** Midday plant water potential for non-infected and infected pine branches measured on spring (A) and summer (B). Panels C, D and E show, respectively, the values of water potential gradient ( $[\Psi]$ ), recalculated in-situ leaf transpiration rate ( $E$ ), and plant conductance ( $k$ ) for non-infected pine (orange), infected pine branches (grey) and mistletoe (blue), during spring and summer. Data are means  $\pm$  s.e. (n=4). Asterisks indicate statistically significant differences across plant material types. ns, not significant. Letters indicate statistically significant differences across seasons (Tukey test,  $P < 0.05$ ).



### Hosted file

image7.emf available at <https://authorea.com/users/817787/articles/1284115-viscum-album-shares-hydraulic-traits-but-causes-a-water-uncoupling-despite-the-adjustments-of-its-host-pinus-sylvestris>

**Fig. 7** Branch transpiration rate ( $E_{branch}$ ) plotted as a function of hydraulic conductivity ( $K_h$ ) for non-infected and infected pine branches (pre- and post- mistletoe insertion) in spring (A) and summer (C). Relationships for non-infected branches were adjusted to a linear function. Pink lines indicate the 95% interval of prediction. The difference between measured and predicted  $E_{branch}$  for infected branches measured at mistletoe pre-insertion (Infected<sub>pre</sub>), is plotted as a linear function of the percentage of mistletoe leaf area in panes B (spring) and D (summer).

### Hosted file

image8.emf available at <https://authorea.com/users/817787/articles/1284115-viscum-album-shares-hydraulic-traits-but-causes-a-water-uncoupling-despite-the-adjustments-of-its-host-pinus-sylvestris>

### Supporting Information

Supporting File 1: Figures S1, S2

Supporting File 2: Summary ANOVA tables S1-S4

Supporting File 3: Extended Statistics

Supporting File 4: Full dataset